

# RSC Advances



This is an *Accepted Manuscript*, which has been through the Royal Society of Chemistry peer review process and has been accepted for publication.

*Accepted Manuscripts* are published online shortly after acceptance, before technical editing, formatting and proof reading. Using this free service, authors can make their results available to the community, in citable form, before we publish the edited article. This *Accepted Manuscript* will be replaced by the edited, formatted and paginated article as soon as this is available.

You can find more information about *Accepted Manuscripts* in the [Information for Authors](#).

Please note that technical editing may introduce minor changes to the text and/or graphics, which may alter content. The journal's standard [Terms & Conditions](#) and the [Ethical guidelines](#) still apply. In no event shall the Royal Society of Chemistry be held responsible for any errors or omissions in this *Accepted Manuscript* or any consequences arising from the use of any information it contains.

# Biodiesel production *via* ethanolsysis of jatropha oil using molybdenum impregnated calcium oxide as solid catalyst

Navjot Kaur and Amjad Ali\*

*School of chemistry and biochemistry, Thapar University, Patiala – 147004 (India)*

*Email: amjadali@thapar.edu, amjad\_2kin@yahoo.com*

*Tel: +91-175-2393832. Fax: +91-175-2364498, 2393005*

**Abstract:** Molybdenum impregnated calcium oxide (Mo/CaO) was prepared via wet impregnation method by varying Mo loading (1-5 wt%) and calcination temperature (300-800 °C). Powder X-ray diffraction study of Mo/CaO catalyst supported the homogeneous doping of Mo in CaO as no peak corresponding to molybdenum oxide was obtained. The prepared catalyst was successfully employed for the ethanolsysis of high free fatty acid (up to 18 wt%) containing vegetable oils with ethanol to give > 99% fatty acid ethyl ester (FAEE) yield under the optimal reaction conditions of ethanol to oil molar ratio of 12:1, catalyst concentration of 5 wt% (catalyst/oil) and reaction temperature of 65 °C. The catalyst was recovered and reused five times without significant loss in its activity. The Koros-Nowak criterion test demonstrated that catalytic activity was independent from the mass transport phenomenon. Under optimized reaction conditions the activation energy ( $E_a$ ) for Mo/CaO catalyzed ethanolsysis was found to be 66.02 kJ mol<sup>-1</sup>. Thermodynamic activation parameters of the reactions were evaluated based on activation complex theory (ACT) and obtained values of  $\Delta G^\ddagger = 43.62$  kJ mol<sup>-1</sup>,  $\Delta H^\ddagger = 64.10$  kJ mol<sup>-1</sup> and  $\Delta S^\ddagger = -60.58$  J mol<sup>-1</sup>K<sup>-1</sup> supported unspontaneous, endothermic and associative mechanism of reaction.

## 1. Introduction

Biodiesel, defined as fatty acid alkyl esters, is a renewable, biodegradable, and non-toxic alternate to conventional diesel fuel.<sup>1</sup> The replacement of mineral diesel with biodiesel would be beneficial from environmental point of view, as later fuel do not contain aromatics and sulfur compounds, has high cetane number and high flash point, causes lower emissions of hydrocarbon and CO<sub>x</sub>.<sup>2</sup> In spite of several advantages biodiesel commercialization has not gained required success in many countries mainly due to the non availability of sufficient feedstock and high product cost.<sup>3</sup>

In this context, use of low cost and low quality feed stocks, such as non edible (e.g., jatropha oil and karanja oil) and waste cooking oil for biodiesel production may improve the economical feasibility of biodiesel.<sup>3</sup> However, the production of biodiesel from non-edible oils is challenging especially in presence of homogeneous catalyst due to the presence of unwanted components such as free fatty acid (FFA) and water; causing the catalyst deactivation via undesirable saponification which not only lower the ester yield but also make the product separation extremely difficult due to emulsification.<sup>4</sup> Moreover, huge quantity of industrial effluents are generated during the essential catalyst removal and product refinement step. A possible solution, to circumvent the problems associated with the use of homogeneous catalysts, is the development and application of heterogeneous catalysts for biodiesel production. Heterogeneous catalysts, although less effective in comparison to the homogeneous one, are easy to separate from the reaction mixture, reusable, and expected to produce biodiesel without any metal ion contamination.<sup>5</sup>

Owing to the high reactivity and cost effectiveness in comparison to other long chain alcohols methanol is frequently employed during industrial scale biodiesel production.<sup>6</sup> However, methanol is highly toxic and non renewable as it is mainly derived from non renewable sources such as petroleum refining products. Thus, there is a need to replace methanol with some other non-toxic and renewable alcohol such as ethanol; produced mainly from biomass fermentation.<sup>7</sup> The physicochemical and combustion properties of fatty acid ethyl esters were found almost similar to that of corresponding methyl esters.<sup>8</sup>

In literature, triglyceride methanolysis is frequently studied in presence of heterogeneous catalysts, however, fewer reports are available regarding the application of heterogeneous catalysts for the triglyceride ethanolysis, mainly due to the lesser activity of ethanol and difficulty in separation of ethyl esters from glycerol. In past a variety of heterogeneous catalysts based on CaO, MgO, SrO, ZnO, magnetic-Fe<sub>2</sub>O<sub>3</sub>, SiO<sub>2</sub>, ZrO<sub>2</sub>, Al<sub>2</sub>O<sub>3</sub> and TiO<sub>2</sub> have been employed for the transesterification reaction and CaO being non toxic, less costlier and easily available has been one of the extensively used among them.<sup>9-12</sup> Pure CaO is not only sensitive towards the presence of FFA and moisture contents, but also it is partially soluble in alcohol and glycerol. In order to improve the stability as well as reactivity CaO based mixed metal oxides were prepared and employed for the transesterification reaction.<sup>12</sup> The active centres in mixed oxides could be either oxide ion or impregnated metal oxide or the defect created due to metal impregnation. These catalysts are frequently employed for the methanolysis of a variety of vegetable oils (VOs), but their activity towards ethanolysis is deliberated in limited reports. A few CaO based catalysts employed in literature for the

ethanolysis of vegetable oils includes CaO, Zr/CaO, CaO-La<sub>2</sub>O<sub>3</sub>, calcium zincate and Ca(OCH<sub>2</sub>CH<sub>3</sub>).<sup>13-17</sup> A 90 % conversion at 78 °C reaction temperature during the ethanolysis of groundnut oil was achieved on applying pure CaO as a catalyst.<sup>13</sup> Kim *et al.* reported the application of CaO-La<sub>2</sub>O<sub>3</sub> catalyst for the ethanolysis of soybean oil in presence of a relatively high catalyst loading of 8 wt% to achieve 71.6 % FAEE yield.<sup>15</sup> Liu *et al.* demonstrated a 91.8 % FAEE yield in calcium ethoxide catalyzed ethanolysis of soybean oil.<sup>17</sup> Thus literature reported heterogeneous catalysts for the ethanolysis reactions have utilized mainly edible oil as feedstock and found to be less active as FAEE yield was less than the acceptable limit of 96.5 % and less stable as their reusability is either not reported or catalytic activity was found to decrease upon repeated use. Moreover, in presence of heterogeneous catalyst, thermodynamics and kinetics of VO ethanolysis are not frequently studied.

In present study, to develop a stable and efficient catalyst for the ethanolysis of high FFA containing non edible VOs, Mo supported CaO was prepared *via* impregnation method by varying the molybdenum concentration and calcination temperature. The kinetics and thermodynamic parameters of Mo/CaO catalyzed ethanolysis of jatropha oil was studied under optimized reaction condition.

## 2. Experimental Section

### 2.1. Materials

Ammonium molybdate ((NH<sub>4</sub>)<sub>6</sub>Mo<sub>7</sub>O<sub>24</sub>·4H<sub>2</sub>O), trichloroacetic acid and benzene (HPLC grade) used for Hammett indicator titration, were obtained from Spectrochem Pvt. Ltd. (India). Hexane, ethyl acetate, acetic acid, ethanol, ammonia (all chemicals of analytical grade purity), and silica gel (TLC grade) were obtained from Loba Chemie Ltd. (India) and used as such without further purification. Waste cottonseed oil (WO), cottonseed oil (CO), karanja oil (KO) and jatropha oil (JO) used for the transesterification reactions were purchased from the local market of Patiala and their chemical analysis is provided in Table S1 (ESI).

### 2.2. Characterization

Powder X-ray diffraction (XRD) patterns were recorded over a 2θ range of 5–80° on a PANalytical's X'Pert Pro diffractometer using monochromatic Cu Kα radiation (λ=1.54060 Å). The phases present in the samples were identified with the help of JCPDS (Joint

Committee of the Powder Diffraction Standards) database files. Thermogravimetric analysis (TGA) was recorded on Shemadzu TGA-50 in the temperature range of 40 to 800 °C at a heating rate of 10 °C min<sup>-1</sup> under normal atmosphere. Fourier transform-infrared spectra (FTIR) of the samples were recorded following the ATR method in the wavenumber region of 400–4000 cm<sup>-1</sup> with an Agilent Cary-660 spectrophotometer.

Scanning electron microscopy coupled with energy dispersive X-ray spectrometry (SEM-EDX) was performed on JEOL JSM 6510LV and transmission electron microscopy (TEM) was performed on HITACHI 7500 instruments. The specific surface area of the catalyst was determined by using the adsorption desorption method at 77 K by the standard Brunauer-Emmett-Teller (BET) method using Micromeritics TriStar -3000 surface area analyzer. All samples were degassed at 200 °C for 2 h under a nitrogen atmosphere to remove the physisorbed moisture from the catalyst surface. The binding energy and electronic state of elements present in catalysts were determined by X-ray photoelectron microscopy using KRATOS-AXIS Ultra DLD spectrometer instrument (Kratos Analytical, UK) equipped monochromator alumina source (Al K $\alpha$  radiation;  $h\nu = 1486.69$  eV). The instrument was operated at 10 kV and 15 mA with pass energy of 160 eV and an increment of 1 eV. Samples were taken in powder form, and deposited on carbon tape and degassed for 2 h in XPS chamber to minimize the air contamination at sample surface. To overcome the charging problem, a charge neutralizer of 2 eV was applied and binding energy of C 1s core level (284.6 eV) was taken as a reference.

Fourier transform-nuclear magnetic resonance (FT-NMR) spectra of JO and corresponding esters were recorded on a JEOL ECS-400 (400 MHz) spectrophotometer in CDCl<sub>3</sub> solvent using tetramethyl silane (TMS) as an internal reference.

Gas chromatography-Mass spectroscopy (GC-MS) of FAEEs was performed on Bruker GC-45X coupled with Scion MS-TQ/SQ system. For GC-MS study samples were diluted with hexane and one  $\mu$ L sample solution was injected (injection temperature 250 °C) in GC (15 m  $\times$  0.25 mm  $\times$  0.25 mm RTX -5MS sil capillary column) in split/splitless mode (split ratio 1:20 for 0.01 s). Helium was used as a carrier gas with a flow rate of 1 ml/min. The column temperature was increased from 60 °C to 300 °C with the heating rate of 10 °C/min. The output from the GC column was entered into the ionization chamber of mass spectrometer *via* a transfer line maintained at 260 °C. Mass spectrum (EI 70 eV, ion source temperature 280°C, solvent delay 2.5 min) was scanned in the m/z range of 50-800. The National Institute

of Standard and Test (NIST) library match software was used to identify the individual FAEE.

The metal ion concentration in FAEE and glycerol was estimated by inductively coupled plasma-atomic emission spectroscopy (ICP-AES) on Spectro ARCOS instrument. The basic strength of the catalysts ( $H_{\text{b}}$ ) was measured by Hammett indicator benzene carboxylic acid titration method<sup>18</sup>, using neutral red ( $H_{\text{b}} = 6.8$ ), bromothymol blue ( $H_{\text{b}} = 7.2$ ), phenolphthalein ( $H_{\text{b}} = 9.3$ ), Nile blue ( $H_{\text{b}} = 10.1$ ), tropaeolin-O ( $H_{\text{b}} = 11.1$ ), 2,4-dinitroaniline ( $H_{\text{b}} = 15.0$ ), and 4-nitroaniline ( $H_{\text{b}} = 18.4$ ) as indicators.

### 2.3. Catalyst preparation

A series of molybdenum impregnated CaO was prepared by the wet impregnation method. In a standard preparation method, 10 g of calcium oxide was suspended in 40 mL of deionized water, and to this 10 mL  $(\text{NH}_4)_6\text{Mo}_7\text{O}_{24}\cdot 4\text{H}_2\text{O}$  solution of desired concentration was added and stirred for 4 h. After the molybdenum incorporation over CaO, the slurry was evaporated to dryness at 120 °C for 24 h and finally calcined at 300-800 °C. A series of Mo/CaO samples was prepared by varying the molybdenum concentration 1 to 5 wt% and calcination temperature 300 to 800 °C. Prepared Mo/CaO was abbreviated as xMo/CaO-T, where x and T represent the molybdenum concentration (wt%) and calcination temperature (°C), respectively.

### 2.4. Transesterification reaction and product analysis

Ethanolysis of JO was performed in a 50 mL two-neck round bottom flask equipped with a water bath on hot plate, magnetic stirrer and water-cooled reflux condenser. Initially, 10 g of JO with desired molar concentrations of ethanol and catalyst was added to the flask. The reaction mixture was heated at desired temperature for a specific time. The reaction mixture was allowed to cool down to room temperature and solid catalyst from this was filtered out. Excess ethanol from the liquid phase was rotary evaporated and remaining mixture was left in a separating funnel for 48 h to separate lower glycerol phase from upper FAEE layer. Finally the FAEE composition as well as yield was determined by GC-MS technique.<sup>19</sup> Ethyl esters obtained upon ethanolysis of JO was also characterized by  $^1\text{H}$  and  $^{13}\text{C}$ -NMR techniques<sup>14</sup> as shown in Fig. S1 (ESI).

### 2.5. Catalysts reusability and leaching tests

To examine the reusability of Mo/CaO catalyst, it was employed during six successive reaction cycles under the optimized reaction conditions. Prior to the next reaction cycle, catalyst was separated from the reaction mixture by filtration, washed thoroughly with hexane to remove adsorbed compound from catalyst surface, and finally regenerated at 700 °C calcination temperature.

The concentration of dissolved catalyst into the reaction mixture was investigated by ICP-AES study. To ensure the heterogeneous nature of the catalyst, and to prove that leached metal ion has not acted like a homogeneous catalyst, a hot filtration test was carried out under optimized reaction conditions. During the test, the catalyst was removed from reaction mixture by filtration after 1.5 h of reaction duration, and reactants were heated again for an additional period of 3.5 h.

### 3. Results and Discussion

#### 3.1 Catalyst characterization

**3.1.1 X-ray diffraction study.** Powder XRD patterns of CaO and Mo/CaO containing different molybdenum concentrations in the range of 0-5 wt% at 700 °C calcination temperature are illustrated in Fig. 1(a). The appearance of sharp peaks in diffraction patterns indicates the formation of highly crystalline materials. Commercial CaO used as support material revealed the characteristic diffraction patterns of *cubic*-calcium oxide (JCPDS 82-1691) as a major phase and *hexagonal*-Ca(OH)<sub>2</sub> as a minor phase (JCPDS 84-1275) is also present. Molybdenum impregnation in CaO was not able to initiate the formation of any new phase. No diffraction peak corresponding to molybdenum oxide or any other phase of molybdenum was observed up to 5 wt % Mo loading in CaO. This indicates that Mo has been incorporated into CaO lattice to form a solid solution of molybdenum oxide in calcium oxide. During Mo/CaO catalyst preparation by wet chemical method in aqueous medium reaction between CaO and H<sub>2</sub>O leads to the formation of Ca(OH)<sub>2</sub> in *hexagonal* phase as supported by the XRD pattern of catalyst heated up to 400 °C (Fig. 1(b)). At 500 °C calcination temperature, Ca(OH)<sub>2</sub> decomposition was initiated into CaO phase and hence both CaO and Ca(OH)<sub>2</sub> phases were observed. A further increase in calcination temperature ( $\geq 600$  °C) leads to the formation of a pure *cubic*-CaO phase which indicated the completion of Ca(OH)<sub>2</sub> decomposition. Similar XRD patterns were observed for Mo/CaO calcined up to 800 °C to indicate that an increase in the calcination temperature beyond 600 °C has not initiated any phase change in Mo/CaO.

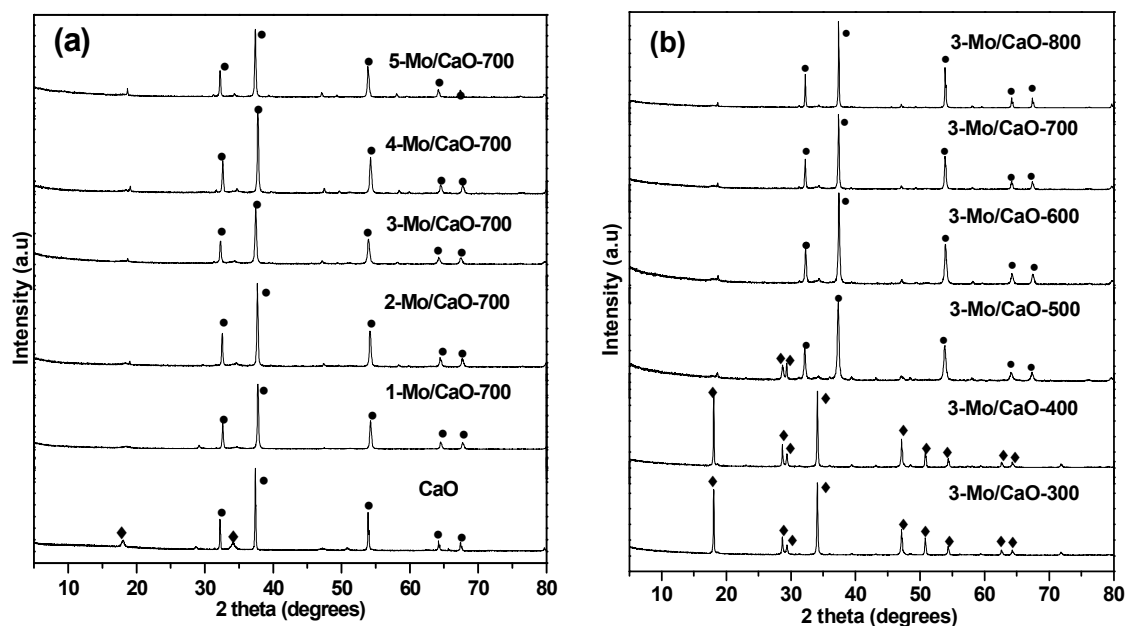


**Fig. 1.** XRD pattern of Mo/CaO with varying (a) Mo concentration (0-5%) and (b) calcination temperature (300-800 °C) (♦ =  $\text{Ca(OH)}_2$ ; • = CaO).

The crystallite size of catalysts at varying Mo loadings and calcination temperature was calculated by Scherrer equation. The catalytic support CaO has crystallite size of 33.0 nm. With increase in molybdenum loading (1-3 wt%) on CaO the crystallite size of the catalyst decreases (33.0-22.5 nm) as shown in Table S2 (ESI). This may be due to the small ionic radius of molybdenum (79 pm) as compared to calcium (114 pm). With increase in calcination temperature (300-500 °C) the crystallite size of the catalyst decreases may be due to the removal of water molecules from the vacant sites of Mo/CaO lattice as well as partial decomposition of  $\text{Ca(OH)}_2$  at 500 °C.<sup>20</sup> Further increase in calcination temperature (600-800 °C) was not found to bring any significant variation in crystallite size as no change in catalyst structure or phase was observed in this temperature range.

**3.1.2. Thermo gravimetric analysis.** TG curve of uncalcined Mo/CaO catalyst is illustrated in Fig. 2, which shows two weight loss regions in the temperature ranges of 437-500 °C and 500-700 °C. The first or major weight loss region (19.22 %) corresponds to the decomposition of  $\text{Ca(OH)}_2$  into CaO phase. The second weight loss region (5.79 %) ascribed to the decomposition of  $\text{CaCO}_3$  which may form due to the reaction of surface CaO with atmospheric  $\text{CO}_2$ . In order to avoid the presence of  $\text{CaCO}_3$ , catalyst was prepared at 700 °C calcination temperature.

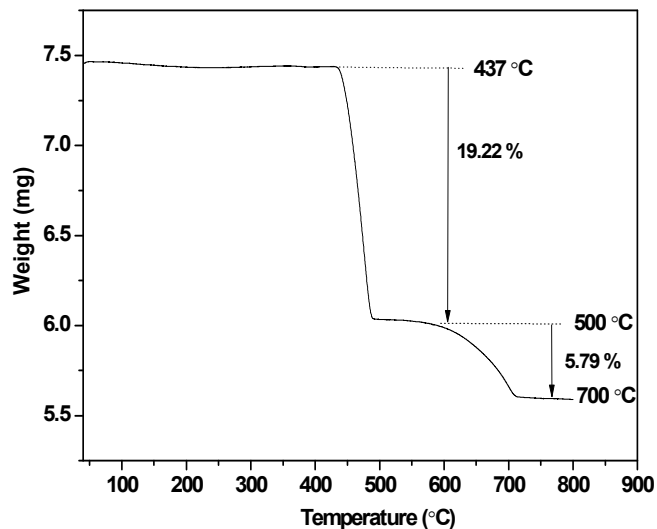


Fig. 2. TG curve of uncalcined 3Mo/CaO catalyst.

**3.1.3. Electron Microscopy studies.** The SEM and TEM images were recorded to determine the morphology and particle size of prepared catalyst. The SEM micrograph shows the clusters of irregular shaped crystalline particles ranging from 0.2-1.0  $\mu\text{m}$  in size which has formed due to the agglomeration of Mo/CaO particles as shown in Fig. 3(a). Qualitative analysis by SEM-EDX study supported the presence of  $\sim 2.7$  wt% Mo in 3-Mo/CaO-700 as shown in Fig. S2 (ESI). TEM image of these particles indicates that each cluster consist of even smaller particles of 25-40 nm size with inconsistent geometries as shown in Fig. 3(b). Thus powder XRD as well as TEM study supported the formation of nano structures of Mo/CaO catalyst.

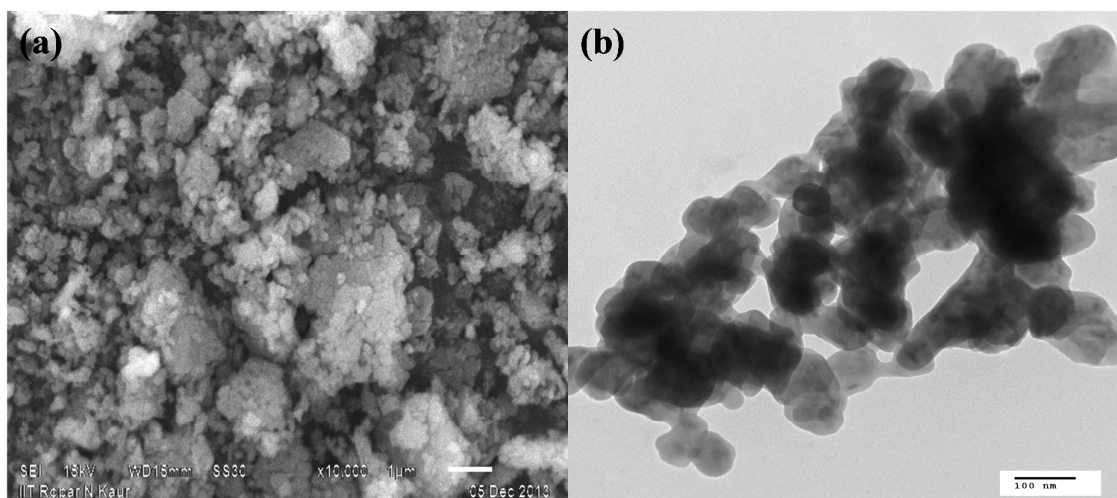


Fig. 3. (a) SEM and (b) TEM image of 3Mo/CaO-700 catalyst.

**3.1.4. BET surface area and porosity measurements.** As given in Table 2, the measured BET surface area of the commercially available CaO was found to be 3.90 m<sup>2</sup>/g and an increase in surface area was observed upon Mo impregnation. It can be clearly seen from Table 1, that the addition of 0-3 wt% molybdenum increases the surface area from 3.90 to 44.29 m<sup>2</sup>/g, however, a further increase of Mo content (up to 5 wt%) resulted in a decrease in surface area. Thus, up to 3 wt% molybdenum dispersed homogeneously into the CaO matrix and a further increase in Mo concentration blocked the micropores of the catalyst. The blockage of pore size is further supported by the larger pore size with 5 wt% Mo loading.

**Table 1.** Surface properties of Mo/CaO catalyst.

Catalyst	Surface area (m <sup>2</sup> /g)	Pore size (nm)	Pore volume (cm <sup>3</sup> /g)
CaO	3.9	N.D	N.D
1-Mo/CaO-700	27.8	32.6	0.22
3-Mo/CaO-700	44.2	20.1	0.22
5-Mo/CaO-700	28.8	28.7	0.20

N.D = Not Determined

The nitrogen adsorption-desorption isotherms (Fig. 4) indicate a type IV isotherm profile for Mo/CaO catalysts at different loading of molybdenum with hysteresis loop H3, at relative pressure of about 0.7-1.0; characteristic to the mesoporous materials.

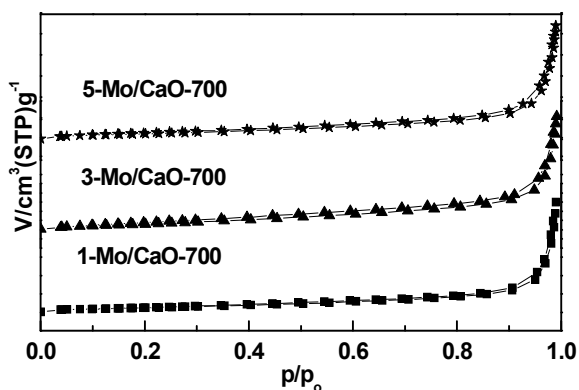


**Fig. 4.** N<sub>2</sub> adsorption-desorption isotherms for Mo/CaO catalyst at varying molybdenum loading.

**3.1.5. XPS analysis.** The electronic state of the metal ions present in catalyst was determined by XPS analysis as shown in Fig. 5. The peaks corresponding to O<sup>2-</sup> (1s), Ca<sup>2+</sup> (2p) and Mo<sup>6+</sup> (3d) were observed at 533, 351 and 231 eV, respectively.<sup>21</sup> Thus XPS study supported the presence of molybdenum over catalyst surface, although same could not be detected by XRD study due to the homogeneous solid solution formation of molybdenum in calcium oxide.

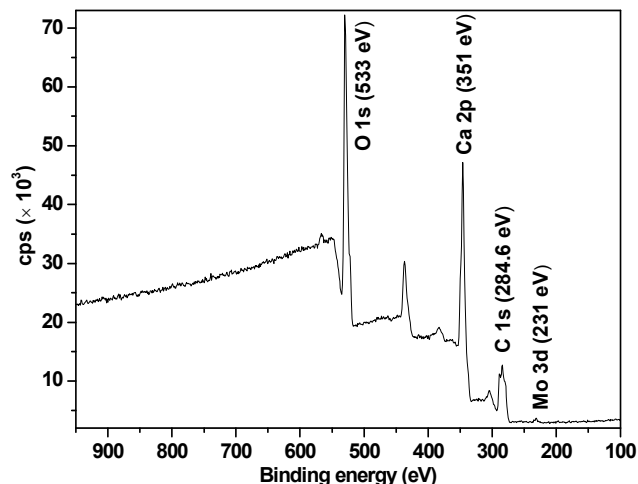


Fig. 5. Wide scan XPS spectra of 3Mo/CaO-700.

### 3.2. Catalytic activity

The commercially available CaO was found to show poor activity towards the ethanolysis of non-edible oils and hence, required relatively longer reaction duration ( $> 10$  h) to achieve the equilibrium. Moreover, due to relatively high solubility of CaO in alcohol biodiesel must be washed to remove the dissolved catalyst.<sup>1</sup> The activity as well as stability of CaO was improved upon molybdenum impregnation. As shown in Table 2, with the increase in molybdenum loading from 1 to 3 wt% at 700 °C calcination temperature, the catalytic activity (TOF) was found to increase due to the increase in catalyst basic sites as well as surface area. A further increase in molybdenum concentration was not found to increase the basic sites and hence, no gain in activity was observed.

The optimized calcination temperature for the catalytic activity was established by preparing the catalyst in the range of 300-800 °C calcination temperature. Up to 400 °C, Bronsted site predominated in the catalyst due to the presence of  $\text{Ca}(\text{OH})_2$  and at  $\geq 600$  °C, these sites converted into Lewis site due to the decomposition of  $\text{Ca}(\text{OH})_2$  into CaO. Transesterification reaction could be effectively catalyzed by Lewis base sites rather than Bronsted sites.<sup>23</sup> In order to remove the possibility of active site blockage due to  $\text{CaCO}_3$  formation, the catalyst was prepared at 700 °C calcination temperature, although its activity as well as basic site strength was found to be similar to the catalyst prepared at 600 °C (Table 2).

**Table 2.** Comparison of basicity and TOF of Mo/CaO at varying loadings of molybdenum and calcination temperature.

Catalyst	Basicity under different indicators (mmol/g of catalyst)					$f_m$ (mmol/g of catalyst)	TOF ( $h^{-1}$ )
	Neutral red $pK_{BH^+}=6.8$	Bromothym -ol blue $pK_{BH^+}=7.2$	Phenolphth- alein $pK_{BH^+}=9.3$	Nile blue $pK_{BH^+}=10.1$	Trapeolin $pK_{BH^+}=11.1$		
CaO	0.28	0.22	0.10	0.14	-	0.74	0.95
1Mo/CaO-700	0.58	0.47	0.25	0.35	-	1.65	1.35
2Mo/CaO-700	1.34	0.82	0.50	0.48	0.73	3.87	2.47
3Mo/CaO-700	1.56	1.40	1.28	0.56	1.04	5.84	3.05
4Mo/CaO-700	1.54	1.42	1.29	0.56	1.02	5.80	3.03
5Mo/CaO-700	1.51	1.43	1.27	0.52	1.00	5.76	3.00
3Mo/CaO-300	0.32	0.25	0.14	0.17	-	0.88	1.12
3Mo/CaO-400	0.59	0.48	0.27	0.38	-	1.72	1.81
3Mo/CaO-500	1.00	0.70	0.57	0.43	0.64	3.34	2.79
3Mo/CaO-600	1.53	1.43	1.26	0.57	1.01	5.80	3.02
3Mo/CaO-800	1.55	1.42	1.26	0.57	1.03	5.83	3.03

TOF =  $\text{mol}_{\text{actual}} / (f_m \times m_{\text{cat}} \times t)$  where  $\text{mol}_{\text{actual}}$ ,  $m_{\text{cat}}$ ,  $t$  and  $f_m$  were the moles of FAEE, mass of catalyst, reaction time and total basicity of catalyst (in mmol/g of catalyst).<sup>22</sup> **Reaction conditions:-** ethanol to oil molar ratio of 12:1 at 65 °C in presence of 5 wt% catalyst (catalyst/oil).

The catalyst prepared with 3 wt% molybdenum loading at 700 °C calcination temperature was found to be most active and hence selected for detailed study.

### 3.3. Mass transfer limitation study

Vegetable oils and ethanol are completely immiscible and hence mass transfer limitations could affect the FAEE yield.<sup>24</sup> To establish the stirring speed at which the mass transfer limitations are minimal during 3Mo/CaO-700 catalyzed transesterification reaction, a series of ethanolysis reaction was performed at 50-650 rpm stirring speed. As could be seen from Fig. 6, initially the reaction rate increases with the increase in stirring speed and at  $\geq 450$  rpm the reaction rate was found to be maximum and constant. Thus all experiments in present study were carried out at a stirring speed of 450 rpm to exclude the effect of mass transfer phenomenon on reaction rate.

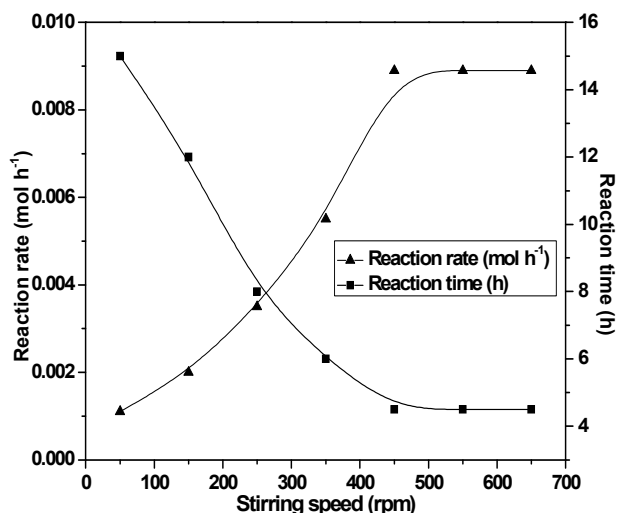


**Fig. 6.** Effect of stirring speed on 3Mo/CaO-700 catalyzed transesterification of JO. **Reaction conditions:-** ethanol to oil molar ratio of 12:1 at 65 °C in presence of 5 wt% catalyst (catalyst/oil).

### 3.4. Effect of the reaction parameters

To optimize the reaction parameters for the better catalytic activity, transesterification reactions were conducted by varying catalyst concentration (1-6 wt%), ethanol to oil molar ratio (3:1-15:1) and reaction temperature (35-75 °C). The detailed experimental procedures of these experiments are provided in Fig. S3 (ESI) and on the basis of this study, a 12:1 ethanol to oil molar ratio at 65 °C reaction temperature, 5 wt% catalyst (with respect to oil) and 4.5 h of reaction duration were found to be the optimum conditions for the 3Mo/CaO-700 catalyzed transesterification of JO.

A comparison between the ethanolysis activity of 3Mo/CaO-700 catalyst and few literature reported catalysts is given in Table 3.

**Table 3.** Comparison of reaction conditions of literature reported heterogeneous catalysts used for ethanolysis with our catalyst.

Catalyst	Oil	Reaction conditions						Ref.
		Catalyst dosage (wt%)	Reaction temp. (°C)	Ethanol to oil molar ratio	Reaction time (h)	FAEE yield (%)	Reusability (FAEE yield after last run)	
CaO	Sunflower	20	75	18:1	6	100	N.R.	13
Zr/CaO	Jatropha	5	75	21:1	7	> 99	N.R.	14
CaO-La <sub>2</sub> O <sub>3</sub>	Soybean	8	65	10:1	6	71.6	N.R.	15
Calcium zincate	Sunflower	3	78	20:1	3	> 95	3 (40)	16
Ca(OCH <sub>2</sub> CH <sub>3</sub> )	Soybean	3	75	12:1	3	91.8	N.R.	17
Sr:Zr	Waste cotton seed	5	75	12:1	7	> 99	4 (98)	22
Mg <sub>2</sub> CoAl <sup>a</sup>	Rapeseed	2	200	16:1	18	97	7 (97)	25
MgO/SBA-15 <sup>a</sup>	Edible oil	2	220	6:1	5	96	N.R.	26
SO <sub>4</sub> <sup>2-</sup> /ZrO <sub>2</sub> <sup>a</sup>	Soybean	5	120	20:1	1	92	4 (15)	27
Li/ZrO <sub>2</sub>	Waste cotton seed	5	75	15:1	4.5	99	9 (90)	28
Mo/CaO	Jatropha	5	65	12:1	4.5	> 99	5 (98)	In present work

N.R – Not reported; <sup>a</sup> – under high pressure in parr batch reactor

As could be seen from the Table 3, Mo/CaO catalyzed ethanolysis of JO required lesser ethanol to oil molar ratio and lower reaction temperature for achieving > 99 % FAEE yield. Moreover, most of the literature reported catalysts either not demonstrated any reusability or showed poor reusability. On the other hand, the catalyst reported in present work has maintained greater than 98% FAEE yield during 5 catalytic runs.

### 3.5. Tolerance towards water and FFA

The presence of water and FFA in case of low quality feedstock, such as nonedible or waste cooking oils, is inevitable although both are found to deactivate the homogeneous base catalysts *via* saponification in traditional biodiesel production processes.<sup>23</sup> Formation of soap would emulsify with reaction mixture, which make the separation of fatty acid ester, glycerol and catalyst extremely difficult.<sup>29</sup>

In order to examine the moisture tolerance of catalyst, transesterification reaction of JO was performed in presence of 0.5-6.5 wt% water contents (with respect to oil). Fig. 7(a) indicates that up to 2.5 wt% addition of water was not found to make any negative effect on catalyst activity. A further increase in water (3.0-6.5 wt%) was found to reduce the catalyst activity due to the change of Lewis basic sites (–O–) into Bronsted basic sites (–OH) due to the reaction of water molecules with catalyst. The Bronsted basic sites were found to be less active towards the transesterification than corresponding Lewis basic sites. A comparison of XRD patterns (Fig. 7(b)) of fresh catalyst with the catalyst exposed to moisture also supported the conversion of CaO phase into Ca(OH)<sub>2</sub> phase.

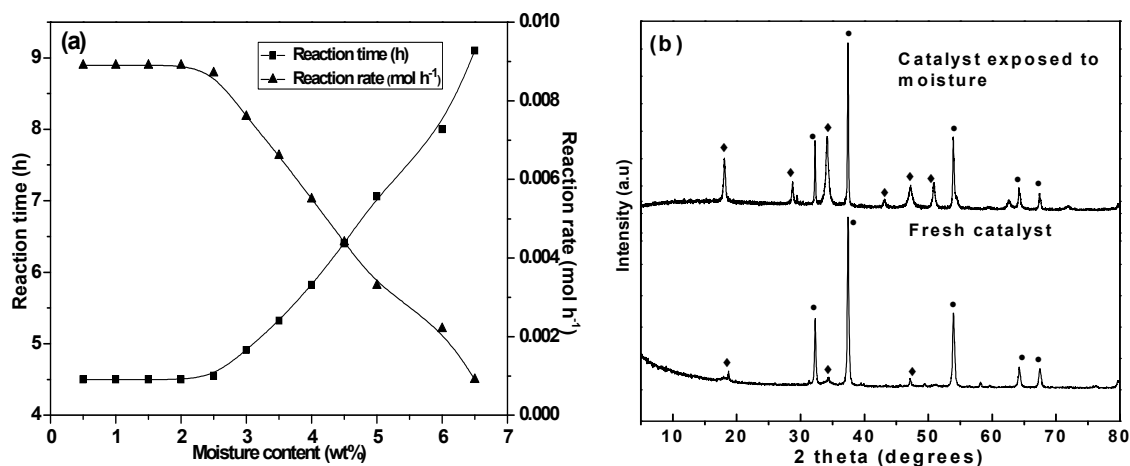


**Fig.7.** (a) Effect of moisture content on the 3Mo/CaO-700 catalyzed transesterification of WO (reaction time is the time required to achieve > 99% FAEE yield) (b) Comparison of XRD spectra of fresh catalyst and catalyst exposed to moisture (● = CaO, ◆ = Ca(OH)<sub>2</sub>).

FFA content in oils not only deactivates the homogeneous alkali catalyst *via* saponification but also found to reduce the activity of heterogeneous catalysts.<sup>23</sup> To evaluate the effect of presence of FFA on 3Mo/CaO-700 activity, transesterification of VO's containing up to 18.1 wt% FFA was performed and results are shown in Fig. 8. The activity of the catalyst was found to decrease as FFA content in oil increases, nevertheless > 99% FAEE yield could be maintained by increasing the reaction duration. The reduction in catalytic activity could be attributed to the strong interaction of highly polar acetate group (of fatty acid) with the catalyst surface (Ca<sup>2+</sup>) to result the partial blocking of the active sites.<sup>27</sup>

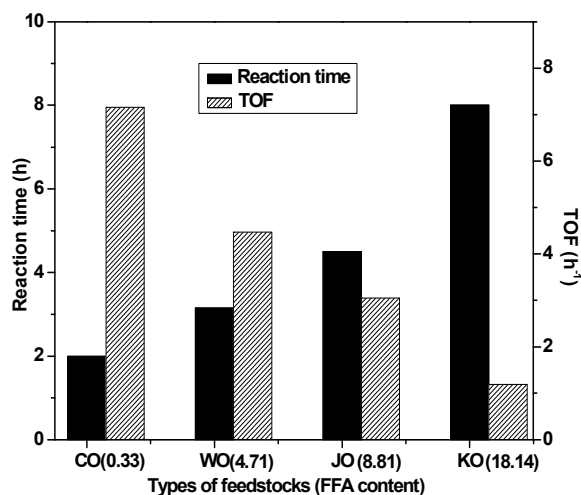


**Fig. 8.** Effect of FFA contents on the 3Mo/CaO-700 catalyzed transesterification of different feed stocks (reaction time is the time required to achieve > 99% FAEE yield). **Reaction conditions:-** Ethanol to oil molar ratio of 12:1 at 65 °C reaction temperature in presence of 5 wt% (catalyst/oil) catalyst.

### 3.6. Reusability and stability

Reusability and ease of separation from the reaction mixture are few important advantages of a heterogeneous catalyst over homogeneous one. As shown in Fig. 9, the catalyst could be reused up to five times without significant loss in activity, however, in sixth run only partial conversion was achieved.

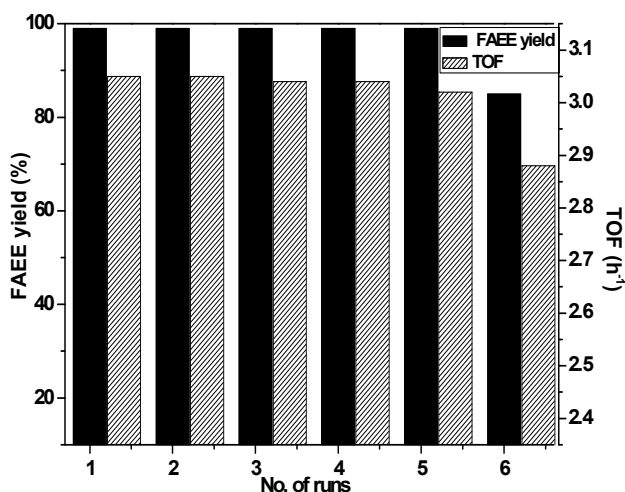


Fig. 9. Reusability study of catalyst.

A comparison of IR spectrum (Fig. S4; ESI) of the fresh and used catalyst rule out the possibility of adsorption of organic molecule over the catalyst surface, which otherwise was found to reduce the catalytic activity.<sup>4</sup> Change in catalyst structure, upon repeated use and activation, could be another reason for the loss of activity. The XRD study (Fig. 10) of fresh and used catalyst validated that upon repeated use CaO phase has partially changed into Ca(OH)<sub>2</sub>.

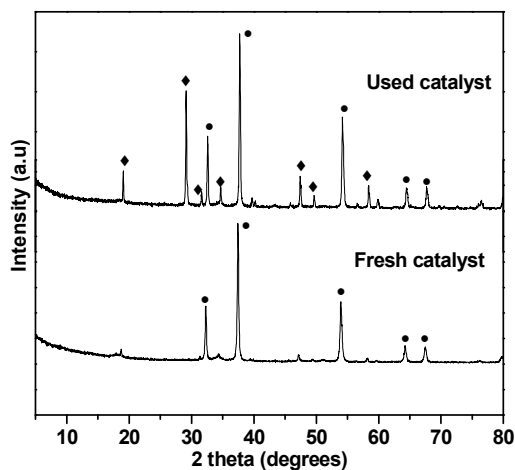


Fig. 10. Comparison of XRD of fresh and used catalyst. (● = CaO, ◆ = Ca(OH)<sub>2</sub>).

The metal analysis supported minute leaching of Mo and Ca in FAEE (1.23 and 0.25 ppm, respectively) as well as in glycerol (4.12 and 2.28 ppm, respectively). Thus catalyst is stable although small amount of metal is lost during the catalytic run, which could be another reason for the loss of activity. To validate that dissolved metal ions have not acted as homogeneous catalyst, hot filtration test was performed (Fig. 11). No significant gain in FAEE yield was obtained when the reaction was continued after filtering out the catalyst to rule out the possibility of homogeneous contribution in catalytic activity by the leached metal ions and to support a truly heterogeneous mode of action of Mo/CaO catalyst.

Therefore, the gradual loss of the catalytic activity could be attributed to (i) structural changes in catalyst and (ii) partial loss of the Mo and Ca from 3Mo/CaO-700 upon its repeated use.

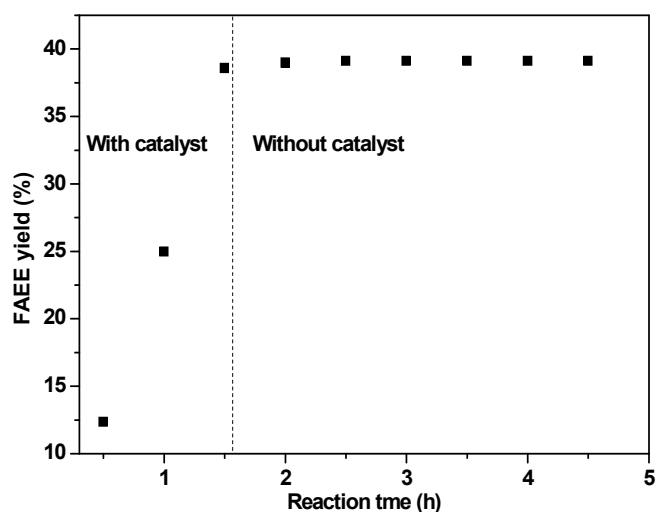


Fig. 11. Hot filtration test for 3Mo/CaO-700 catalyzed transesterification.

### 3.7. Kinetics and thermodynamic studies

Transesterification is generally assumed to follow pseudo-first-order kinetics as alcohol in such reactions are employed in excess to the required stoichiometric amount of 3:1 alcohol to oil molar ratio.<sup>30</sup> In this study, ethyl esters yield with respect to time was followed (Fig. S5) to study the reaction kinetics by performing the reaction under optimized reaction conditions. Since a 12:1 ethanol to oil molar ratio was employed, the kinetics of 3Mo/CaO-700 catalyzed ethanolysis could safely be assumed to follow (pseudo) first order<sup>30</sup> equation 1:

$$-\ln(1-X) = k t \quad (1)$$

where  $k$  is the first order rate constant,  $X$  is the amount of oil converted into FAEE.

The linear nature of  $-\ln(1-X)$  versus  $t$  plot supported that the reaction has followed the (pseudo) first order rate law (Fig. 12(a)). The apparent first order rate constant from the plot was observed  $1.01 \text{ h}^{-1}$  at  $65 \text{ }^\circ\text{C}$ .

To calculate the activation energy, reactions were carried out in the temperatures range of  $35\text{--}65 \text{ }^\circ\text{C}$ . The Arrhenius equation 2 was employed<sup>31</sup> to estimate the activation energy ( $E_a$ ) and pre-exponential factor ( $A$ ).

$$\ln k = \ln A - E_a/RT \quad (2)$$

where  $E_a$  is the activation energy ( $\text{kJ mol}^{-1}$ ),  $A$  is the pre-exponential factor ( $\text{h}^{-1}$ ),  $R$  is the gas constant ( $8.314 \times 10^{-3} \text{ kJ K}^{-1} \text{ mol}^{-1}$ ) and  $T$  is the reaction temperature ( $^\circ\text{K}$ ).

The values of  $E_a$  and  $A$  from  $\ln k$  versus  $1/T$  plot (Fig. 12(b)) were found to be  $66.02 \text{ kJ mol}^{-1}$  and  $9.2 \times 10^9 \text{ h}^{-1}$ , respectively.

The observed  $E_a$  value in present study ( $66.02 \text{ kJ mol}^{-1}$ ) was found within the range of reported values ( $26\text{--}82 \text{ kJ mol}^{-1}$ ) for transesterification reaction catalyzed by heterogeneous catalysts.<sup>14</sup> A value of  $E_a > 25 \text{ kJ mol}^{-1}$  also supported that  $3\text{Mo}/\text{CaO}\text{-}700$  catalyzed transesterification is a chemically controlled reaction and not controlled by mass transfer limitations.<sup>32</sup>

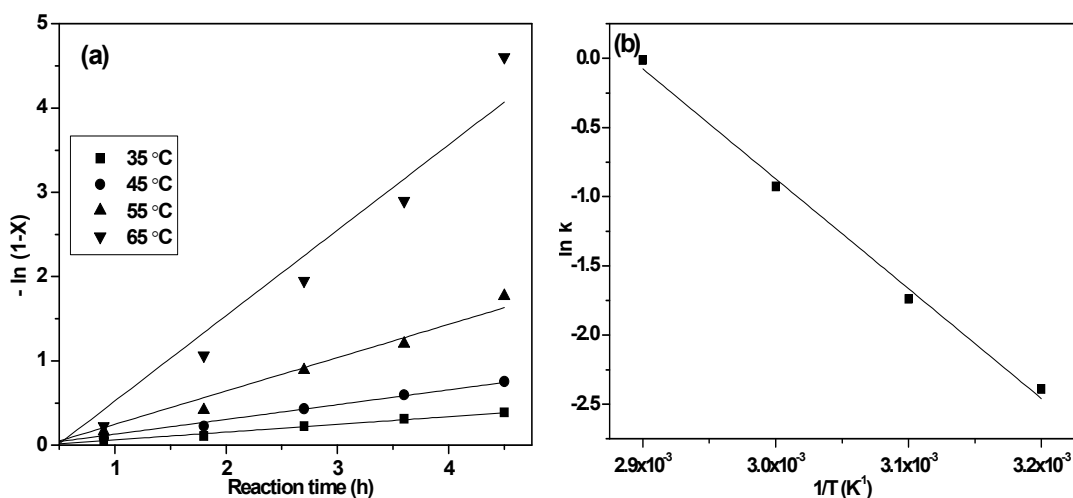


**Fig.12.** Kinetic study of transesterification of JO with ethanol over  $3\text{Mo}/\text{CaO}\text{-}700$  catalyst. (a) Plots of  $-\ln(1-X)$  vs time at different temperatures (b) Arrhenius plot of  $\ln k$  vs  $1/T$ . **Reaction conditions:** ethanol to oil molar ratio of 12:1 and 5 wt% of  $3\text{Mo}/\text{CaO}\text{-}700$  with respect to oil.

The thermodynamic parameters such as enthalpy ( $\Delta H^\ddagger$ ) and entropy ( $\Delta S^\ddagger$ ), were not frequently studied for the transesterification reactions catalyzed by heterogeneous catalyst. In present study to evaluate these parameters Eyring equation 4 was applied.<sup>33</sup>

$$\ln\left(\frac{k}{T}\right) = -\frac{\Delta H^\ddagger}{R}\left(\frac{1}{T}\right) + \left[\ln\left(\frac{k_B}{h}\right) + \frac{\Delta S^\ddagger}{R}\right] \quad (4)$$

where  $k_B$  and  $h$  are the Boltzmann ( $1.38 \times 10^{-23} \text{ J K}^{-1}$ ) and Planck ( $6.63 \times 10^{-34} \text{ Js}$ ) constants, respectively.

Equation 4 resembles van't Hoff's equation describing the mathematical relation between enthalpy and entropy of activation with rate constant. The superscript  $\ddagger$  notation refers to the value of interest in the activation complex or transition state. The slope and intercept of  $1/T$  versus  $\ln(k/T)$  plot would be equals to  $-\Delta H^\ddagger/R$  and  $\ln(k_B/h) + \Delta S^\ddagger/R$ , respectively.

Fig. 13 depicts the Eyring plot of Mo/CaO catalyzed transesterification of JO and from this plot the value of  $\Delta H^\ddagger$  was found to be  $64.10 \text{ kJ mol}^{-1}$ . The positive value indicates that reaction is endothermic and thus an external heating source is needed to raise the energy level of reactants so that they could be transformed to the transition state. The value of  $\Delta S^\ddagger$  was found to be negative ( $-60.58 \text{ J mol}^{-1}\text{K}^{-1}$ ) to suggest that associative mechanism is followed in which reactant species might have joined together over catalyst surface to form a more ordered transition state.

The Gibb's free energy of activation ( $\Delta G^\ddagger$ ) was determined at  $65 \text{ }^\circ\text{C}$  from fundamental thermodynamics equation 5.<sup>34</sup>

$$\Delta G^\ddagger = \Delta H^\ddagger - T\Delta S^\ddagger \quad (5)$$

The  $\Delta G^\ddagger$  value was found to be  $43.62 \text{ kJ mol}^{-1}$ , to indicate unspontaneous nature of the reaction in which transition state is having higher energy level than reactants.

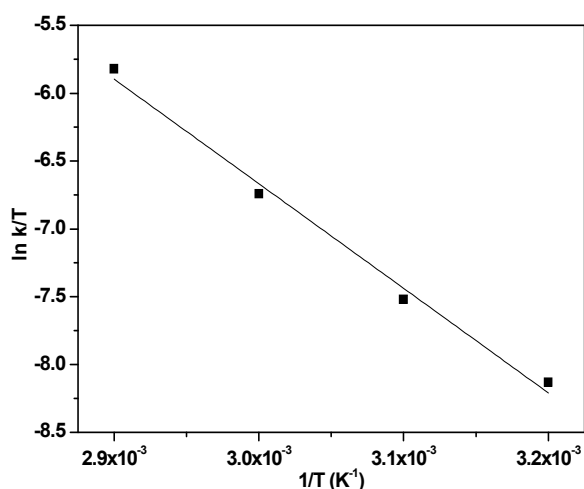
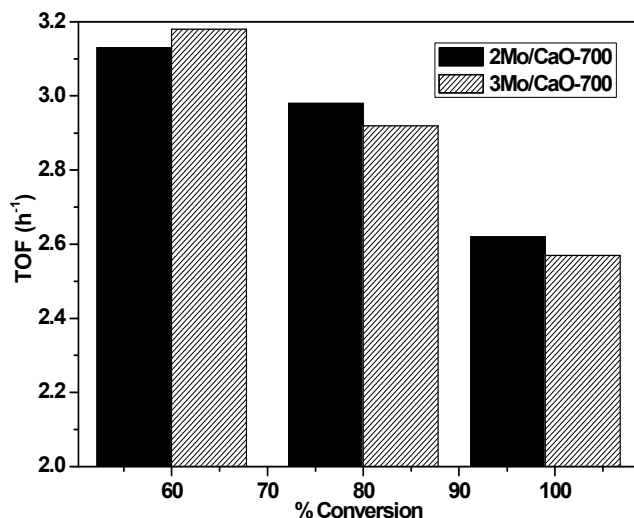


Fig. 13. The Eyring plot of 3Mo/CaO-700 catalyzed transesterification of JO.

### 3.8. Koros–Nowak Criterion test

Koros–Nowak criterion test was performed to find out whether reaction rates were free from mass transfer effects.<sup>30,35</sup> In present study the reactions were carried out in presence of two catalysts in which concentration of active sites over the catalyst has been changed without changing the total active (basic) sites. As shown in Fig. 14, at similar conversion levels, TOFs of both the catalysts were found to be almost similar to prove the absence of mass diffusion limitations in Mo/CaO catalyzed reaction.



**Fig. 14.** A plot of TOF vs % conversion for the 2Mo/CaO-700 and 3Mo/CaO-700 catalyzed ethanolsis of JO. **Reaction conditions:** ethanol to oil molar ratio; 12:1 at 65 °C and catalyst concentration; either 5 wt% of 3Mo/CaO-700 or 7.5 wt% of 2Mo/CaO-700.

### 3.9. Fuel properties of biodiesel

Physicochemical properties of the biodiesel depend upon their fatty acid composition which could be evaluated by GC-MS study. Gas chromatogram of FAEE prepared from JO is provided in Fig. S6 (ESI) and corresponding fatty acid ester composition is listed in Table 4. Total FAEE content was observed as high as 99.37 wt%, consisting of 26.66 wt% saturated and 72.71 wt% unsaturated fatty acid esters. A high percentage of unsaturated fatty acid ester indicates better cold flow properties of biodiesel even at low temperature.<sup>36</sup>

**Table 4.** Composition of JO derived FAEE.

S.No.	Retention time (min)	Composition; Molecular formula	Corresponding acid (Cx:y)	Wt %
1	3.93	Caprylic acid ethyl ester; C <sub>10</sub> H <sub>20</sub> O <sub>2</sub>	Caprylic acid (C8:0)	0.24
2	5.99	Pelargonic acid ethyl ester; C <sub>11</sub> H <sub>22</sub> O <sub>2</sub>	Pelargonic acid (C9:0)	0.36
3	8.57	Palmitoleic acid ethyl ester; C <sub>18</sub> H <sub>34</sub> O <sub>2</sub>	Palmitoleic acid (C16:1)	1.04
4	8.68	Palmitic acid ethyl ester; C <sub>18</sub> H <sub>36</sub> O <sub>2</sub>	Palmitic acid (C16:0)	18.04
5	9.47	Linoleic acid ethyl ester; C <sub>20</sub> H <sub>36</sub> O <sub>2</sub>	Linoleic acid (C18:2)	20.36
6	9.49	Oleic acid ethyl ester; C <sub>20</sub> H <sub>38</sub> O <sub>2</sub>	Oleic acid (C18:1)	50.67
7	9.61	Stearic acid ethyl ester; C <sub>20</sub> H <sub>40</sub> O <sub>2</sub>	Stearic acid (C18:0)	8.02
8	11.03	Linolenic acid ethyl ester; C <sub>20</sub> H <sub>34</sub> O <sub>2</sub>	Linolenic acid (C20:3)	0.64

x:y = number of carbon atoms:number of double bonds

Few more fuel properties of prepared FAEE were studied and compared with the European specifications EN 14214. As could be seen from Table 5, the observed values of properties for the prepared biodiesel fuel were found within the acceptable limits of European standards.

**Table 5.** Fuel properties of the FAEE prepared from JO.

S.No.	Parameters	Units	FAEE	EN 14214	Test method
1	Flash point	°C	120	100–170	ASTM D93
2	Pour point	°C	0	–5 to10	ASTM D2500
3	Kinematic viscosity at 40 °C	cSt	4.92	1.9–6.0	ASTM D445
4	Density at 31 °C	kg/mm <sup>3</sup>	883	860–900	ISI448 P:32
5	Moisture content	%	0.28	≤ 0.5	ASTM D2709
6	Ash	%	0.01	0.02	ASTM D874
7	Iodine value	mg of I <sub>2</sub> /g of sample	89.8	≤ 120	<sup>1</sup> H-NMR <sup>33</sup>
8	Acid value	mg of KOH/g of sample	0.45	0.8	ASTM D664
9	Saponification value	mg of KOH/g of sample	183.49	–	ASTM D5558
10	Ester content	%	> 99 %	≥ 96.5	<sup>1</sup> H-NMR,GC-MS
11	Mo/Ca	ppm	1.23/0.25	≤5 (Total metal)	ICP-AES

#### 4. Conclusions

Molybdenum impregnated calcium oxide has been synthesized *via* wet impregnation method and found effective for the ethanolysis of non edible oils having FFA contents as high as 18.1 wt%. The prepared catalyst under mild reaction conditions (Reaction temperature 65 °C, catalyst amount 5 wt% and ethanol to oil molar ratio 12:1) demonstrated > 99 % FAEE yield in 4.5 h of reaction duration with lesser leaching of Mo and Ca in the reaction mixture and was found to be reusable during 5 catalytic runs. The Koros-Nowak test and mass transfer limitation study demonstrate that catalytic activity was independent from the diffusion limitations. The values of thermodynamic activation parameters  $\Delta G^\ddagger$ ,  $\Delta H^\ddagger$  and  $\Delta S^\ddagger$  were

found out to be  $43.62 \text{ kJ mol}^{-1}$ ,  $64.10 \text{ kJ mol}^{-1}$  and  $-60.58 \text{ J mol}^{-1}\text{K}^{-1}$ , respectively, which show that reaction was unspontaneous, endothermic and endergonic in nature.

### Acknowledgements

We acknowledge CSIR (01(2503)/11/EMR-II) and DRDO (ERIP/ER/1103933/M/01/1453) for the financial support. School of Chemistry and Biochemistry (Thapar University, Patiala) acknowledges DST-FIST grant for GC-MS facility. We are thankful to SAIF (Panjab University, Chandigarh) for powder XRD, TEM and FT-IR, IIT Ropar (Ropar) for SEM, SAI laboratories (Thapar University, Patiala) for NMR, and Avansa Technology and services, Kanpur for surface area analysis. We are also thankful to Dr. Nitin Kumar Singhal (NABI, Mohali) for ICP-AES study.

### References

1. S. H. Teo, U. Rashid and Y. H. T. Yap, *Fuel*, 2014, **136**, 244.
2. Q. Liu, B. Wang, C. Wang, Z. Tian, W. Qu, H. Ma and R. Xu, *Green Chem.*, 2014, **16**, 2604.
3. S. H. Teo, Y. H. T. Yap and F. L. Ng, *Energy Convers. Manage.*, 2014, doi: 10.1016/j.enconman.2014.04.049.
4. D. Singh, R. Bhoi, A. Ganesh and S. Mahajani, *Energy Fuel*, 2014, **28**, 2743.
5. E. Rashtizadeh, F. Farzaneh and Z. Talebpour, *Bioresour. Technol.*, 2014, **154**, 32.
6. C. Brunshwig, W. Moussavou and J. Blin, *Prog. Energ. Combust. Sci.*, 2012, **38**, 283.
7. N. S. Gerhard, T. M. F. S. Vieira, S. S. Groppo, J. R. Rodrigues and M. A. B. R. Arce, *Fuel*, 2014, **116**, 415.
8. O. S. Stamenkovic, A. V. Velickovic and V. B. Veljkovic, *Fuel*, 2011, **90**, 3141.
9. S. Tang, L. Wang, Y. Zhang, S. Li., S. Tian and B. Wang, *Fuel Process. Technol.*, 2012, **95**, 84.
10. H. J. Kim, B. S. Kang, M. J. Kim, Y. M. Park, D. K. Kim, J. S. Lee and K. Y. Lee, *Catal. Today*, 2004, **93–95**, 315.
11. T. Wan, P. Yu, S. Wang, and Y. Luo, *Energy Fuel*, 2009, **23**, 1089.
12. C. Ngamcharussrivichai, P. Totarat and K. Bunyakiat, *Appl Catal A Gen.*, 2008, **341**, 77.
13. H. K. Phiri, Y. Matsumura, T. Minowa and S. Fujimoto, *J. Jpn. Inst. Energy*, 2010, **89**, 53.

14. N. Kaur and A. Ali, *Fuel Process. Technol.*, 2014, **119**, 173.
15. M. Kim, C. D. Maggio, S. Yan, S. O. Salley and K. Y. S. Ng, *Appl. Catal. A: Gen.*, 2010, **378**, 134.
16. J. M. R. Caballero, J. S. Gonzalez, J. M. Robles, R. M. Tost, M. L. A. Castillo, E. V. Alonso, A. J. Lopez and P. M. Torres, *Fuel*, 2013, **105**, 518.
17. X. Liu, X. Piao, Y. Wang and S. Zhu, *Energy Fuel*, 2008, **22**, 1313.
18. T. Yamanaka and K. Tanabe, *J. Phys. Chem.*, 1975, **79**, 2409.
19. Y. Li, X. D. Zhang, L. Sun, M. Xu, W. G. Zhou and X. H. Liang, *Appl. Energ.*, 2010, **87**, 2369.
20. Y. C. Wong, Y. P. Tan, Y. H. T. Yap and I. Ramli, *Sains Malays.*, 2014, **43**, 783.
21. W. Xie, L. Zhao, *Energy Convers. Manage.*, 2014, **79**, 34.
22. N. Kaur and A. Ali, *RSC Adv.*, 2014, **4**, 43671.
23. S. Yan, M. Kim, S. O. Salley and K. Y. S. Ng, *Appl. Catal. A: Gen.*, 2009, **360**, 163.
24. M. A. Dube, A. Y. Tremblay and J. Liu, *Bioresour. Technol.*, 2007, **98**, 639.
25. E. Li, Z. P. Xu and V. Rudolph, *Appl. Catal. B: Environ.*, 2009, **88**, 42.
26. E. Li and V. Rudolph, *Energy Fuel*, 2008, **22**, 145.
27. C. M. Garcia, S. Teixeira, L. L. Marciniuk and U. Schuchardt, *Bioresour. Technol.*, 2008, **99**, 6608.
28. N. Kaur and A. Ali, *Appl. Catal. A: Gen.*, 2015, **489**, 193.
29. S. Yan, S. O. Salley and K. Y. Simon, *Appl. Catal. A: Gen.*, 2009, **353**, 203.
30. R. Song, D. Tong, J. Tang and C. Hu, *Energy Fuel*, 2011, **25**, 2679.
31. J. M. Balbino, E. W. D. Menezes, E. V. Benvenuti, R. Cataluna, G. Ebelinga and J. Dupont, *Green Chem.*, 2011, **13**, 3111.
32. A. Patel and V. Brahmkhatri, *Fuel Process. Technol.*, 2013, **113**, 141.
33. L. K. Ong, A. Kurniawan, A. C. Suwandi, C. X. Lin, X. S. Zhao and S. Ismadji, *J. Supercrit. Fluids*, 2013, **75**, 11.
34. D. Galvan, J. R. Orives, R. L. Coppo, E. T. Silva, K. G. Angilelli and D. Borsato, *Energy Fuel*, 2013, **27**, 6866.
35. R. J. Madon and M. Boudart, *Ind. Eng. Chem. Fundam.*, 1902, **21**, 438.
36. E. Lotero, Y. Liu, D. E. Lopez, K. Suwannakarn, D. A. Bruce and J. G. Goodwin, *Ind. Eng. Chem. Res.*, 2005, **44**, 5353.

## Biodiesel production *via* ethanolsysis of jatropha oil using molybdenum impregnated calcium oxide as solid catalyst

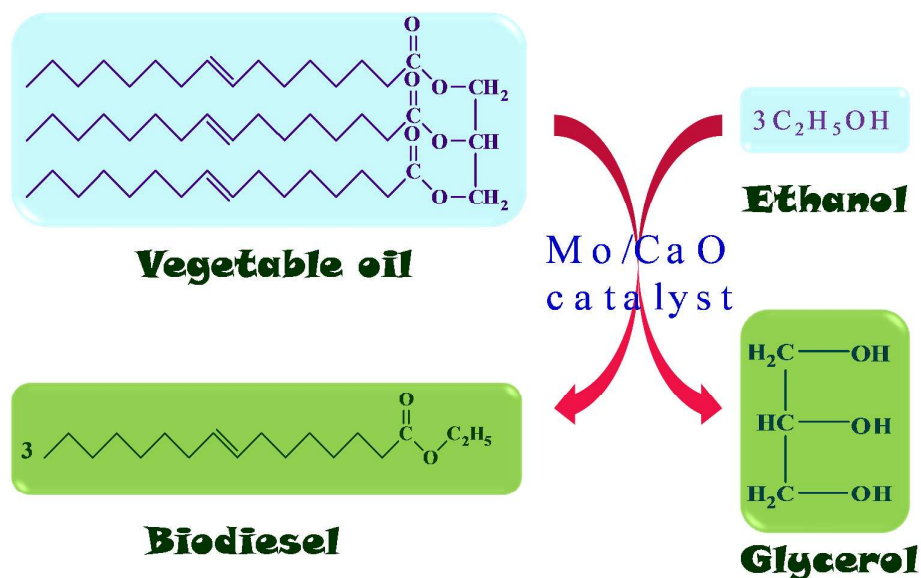
Navjot Kaur and Amjad Ali\*

*School of chemistry and biochemistry, Thapar University, Patiala – 147004 (India)*

*Email: amjadali@thapar.edu, amjad\_2kin@yahoo.com*

*Tel: +91-175-2393832. Fax: +91-175-2364498, 2393005*

### Graphical abstract:



### Textual abstract:

Mo/CaO catalyst was employed for the ethanolsysis of high free fatty acid containing (up to 18 wt%) vegetable oils to produce biodiesel.